EMAIL

estelldatum: 2007-08-23 08:49:53

NORMAL

Kopie SUBITO-2007082300401

nstitut fuer Niedertemperatur-Plasmaphysik
ibliothek
elix-Hausdorff-Strasse 2
7489 Greifswald

Ben.-Gruppe: USER-GROUP-4
Tel: 03834/554 439
Mail: paepke@inp-greifswald.de

Fax: 03834/554 301

Subito-Kundennummer:
SLS02X00252
Subito-Bestellnummer:
SUBITO-2007082300401

4 Z 2003.950 Hbzs 110-42 = Neueste Hefte

ahrgang: 2007

and/Heft: 13

eiten: 351

erfasser: Stancu, Gabi Daniel
ufsatz)

itel: In situ monitoring of silicon ...
ufsatz)

itel:
hemical vapor deposition
SSN: 0948-1907

065953852

A001670566

emerkung:

Beschreibung:

ie Abrechnung dieser Lieferung erfolgt über die subito-Zentralregulierung

ei Rückfragen wenden Sie sich bitte innerhalb von 10 Tagen an die Bayerische Staatsbibliothek, Direktlieferdienste
el. ++49 89 28 638-26 43, doklief@bsb-muenchen.de

Wir weisen den Empfänger darauf hin, dass Sie nach geltendem Urheberrecht die von uns übersandten Vervielfältigungsstücke ausschließlich zu Ihrem privaten oder sonstigen Gebrauch verwenden und weder entgeltlich noch unentgeltlich in Papierform oder als

Chemical Vapor Deposition

DOI: 10.1002/cvde.200606584

Full Paper

In Situ Monitoring of Silicon Plasma Etching Using a Quantum Cascade Laser Arrangement**

By *Gabi Daniel Stancu, Norbert Lang, Jürgen Röpcke,** *Marco Reinicke, Andreas Steinbach,* and *Stephan Wege*

In etch plasmas used for semiconductor processing, concentrations of the precursor gas NF_3 and of the etch product SiF_4 are measured online and in situ using a new diagnostic arrangement, the Q-MACS Etch system, which is based on quantum cascade laser absorption spectroscopy (QCLAS). In addition, the etch rates of SiO_2 layers and of the silicon wafer are monitored including plasma-etching endpoint detection. For this purpose the Q-MACS Etch system is working as an interferometer arrangement. The experiments are performed in an industrial, dual-frequency, capacitively coupled, magnetically enhanced, reactive ion etcher (MERIE), which is a plasma reactor developed for dynamic random access memory (DRAM) technologies. In the spectral range 1028 ± 0.3 cm^{-1}, the absorption cross-sections of SiF_4 and NF_3 are determined to be $\sigma = (7.7 \pm 0.7) \times 10^{-18}$ cm^2 molecule^{-1} and $\sigma = (8.7 \pm 0.8) \times 10^{-20}$ cm^2 molecule^{-1}, respectively.

Keywords: Absorption cross-section, Concentration, Deep trench etching, Infrared absorption, Interferometry, MERIE, NF_3, Plasma etching, QCLAS, Quantum cascade laser, SiF_4

1. Introduction

Molecular plasmas in the low- as well as in the high-pressure range are of increasing importance, not only for fundamental research but also for plasma processing and technology. Thin-film deposition, semiconductor processing, the destruction of toxic compounds, surface cleaning and treatment are established applications of plasmas.

During the last forty years, plasma etching has become a fundamental part of processing of integrated circuits. The optimization of the plasma chemistry of etching processes includes the identification of the mechanisms responsible for plasma-induced surface reactions combined with the achievement of uniformity in the distribution of molecules and radicals for homogeneous wafer treatment.

The necessity of higher packing densities of modern devices requires the reduction in critical lateral dimensions and of layer thicknesses. At present, fabrication technologies of dynamic random access memory (DRAM) are facing critical dimensions below 60 nm and etch aspect ratios of about one hundred. These aspects demand significantly improved knowledge about complex process mechanisms, including the control and monitoring of industrial plasma reactors.

During etching processes, selected areas are removed from the wafer substrates. In the process of semiconductor fabrication two types of etching have been used so far, wet etching and plasma etching. Wet etching is a pure chemical reaction and it has the disadvantage of producing isotropic etch profiles. Due to the increasing chip density, the undercutting effect becomes problematic. Therefore, this technique has been replaced by dry etching which is a plasma-sustained process. Plasma etching provides anisotropic etch profiles. In plasma free radicals and ions are generated which remove material from the area that is uncovered by a pattern mask made, for example, of a photo resist by photolithography.

Therefore, plasma etching has become a very important technology in the production of electronic circuits. The cost reduction of the final product relies on the high reproducibility of the etching processes in the plasma. Thus, in the past, several approaches have been used to study and to monitor plasma-etching processes. Nevertheless, the implementation of diagnostic tools into the production systems is rather complicated due to specific requirements that have to be considered while fulfilling clean room specifications; on-line and in situ monitoring capability, and the non-intrusive character of the method.

Nowadays, in deep trench etch reactors, in situ monitoring of plasma etching is usually performed with optical

[*] Prof. J. Röpcke, Dr. G. D. Stancu, Dr. N. Lang
INP-Greifswald
Felix-Hausdorff-Str. 2, 17489 Greifswald (Germany)
E-mail: roepcke@inp-greifswald.de
M. Reinicke
TU Dresden, IHM
Nöthnitzer-Str. 64, 01187 Dresden (Germany)
Dr. A. Steinbach, S. Wege
Qimonda Dresden, GmbH & Co. OHG
Königsbrücker-Str. 180, 01099 Dresden (Germany)

[**] The authors convey their sincere thanks to S. Barth and U. Macherius for their permanent support and a stimulating working climate. We are also indebted to F. Hempel, S. Glitsch, D. Gött, F. Weichbrodt, and H. Zimmermann for the technical assistance and useful discussions. The work for this paper was supported by the EFRE fund of the European Community and by funding of the State of Saxony of the Federal Republic of Germany, project IGEL, project number 10758/1659.

 © 2007 WILEY-VCH Verlag GmbH & Co. KGaA, Weinheim WILEY InterScience

emission spectroscopy (OES), self-excited electron resonance spectroscopy (SEERS), and mass spectrometry (MS).[1] Generally, the etch performance is analyzed by ex-situ methods, such as gravimetry, scanning electron microscopy (SEM), interferometry, and ellipsometry. On-line monitoring using OES has the advantage of being a non-intrusive and fast measurement method, but it has to be considered that with OES only direct information about the concentration of the excited species can be achieved. In order to obtain ground state concentrations, complex models and calibration methods are necessary. Furthermore, often the species selectivity is not sufficient. Using SEERS, global plasma parameters about the electron component, such as electron density and electron collision rate, can be derived. With MS, concentrations of several species can be monitored, but comprehensive calibration is required for achieving quantitative data. MS is an intrusive method and a high time resolution is difficult to realize. Hence, MS is mainly used in research and development.

Broad-band infrared spectroscopy, in particular Fourier transform infrared (FTIR) spectroscopy, has been used as an approach for investigations of plasma etching and CVD processes. Recently, Grählert et al. analyzed the composition of exhaust gases with the help of a FTIR arrangement in a specially designed measuring cell.[2] These measurements were performed in the exhaust of the process reactor outside of the clean room area. For appropriate sensitivity of the absorption measurements, a liquid nitrogen-cooled detector was used. Although the measuring frequency and spectral resolution were rather low, 0.14 Hz and 1 cm^{-1}, respectively, information about several stable components of the exhaust gas could be achieved.

In the past, few attempts using laser absorption and interferometer techniques were made for on-line monitoring in plasma etch reactors. A laser interferometer using linearly polarized radiation of a He–Ne laser at 632.8 nm for monitoring etching rates in plasma, and controlling the etched depth of isolation areas in silicon for oxide-isolated bipolar devices, has been demonstrated by Sternheim et al.[3] Similar work has been done by Heason and Spencer using tunable, near-infrared lasers.[4] An endpoint detection system for plasma etching based on tunable diode, laser absorption spectroscopy (TDLAS) in the infrared spectral range with lead salt lasers has been described by Sun et al.[5] Lead salt lasers are narrow-band laser sources with the advantage of high spectral intensity, narrow bandwidth, and continuous tunability over the absorption profile. Using TDLAS, Sun et al. monitored the concentration of SiF_4 by measuring its absorption at 1023 cm^{-1}.[5]

The main disadvantage of TDLAS systems, based upon lead salt diode lasers, is the necessary cryogenic cooling of the lasers (and also of the detectors), because they operate at temperatures below 100 K. Systems based upon lead salt diode lasers are typically large in size, and require closed cycle refrigerators and/or cryogens such as liquid nitrogen. The recent development and commercial availability of pulsed quantum cascade lasers (QCL) offers an attractive new option for infrared absorption spectroscopy.[6–9]

Pulsed QCLs are able to emit mid-IR radiation near to room temperature. Compared to lead salt lasers, QCLs allow the realization of very compact mid-infrared sources characterized by narrow line width combining single-frequency operation and considerably higher power values, i.e., of tens of mW. The output power is sufficient to combine them with thermoelectrically cooled infrared detectors, which permits a decrease in the apparatus size and gives a unique opportunity to design compact, liquid nitrogen-free, mid-IR spectroscopic systems. These positive features of QCLAS can open up new fields of application in research and industry, including in situ control of industrial plasma processes.

Recently, a compact QCL measurement and control system (Q-MACS) has been developed for time-resolved plasma diagnostics, process control, and trace gas monitoring, which can be used as a platform for various applications of QCLAS.[10,11]

Based on Q-MACS, a new diagnostic arrangement, the Q-MACS Etch system, has been designed and constructed. In the present paper we demonstrate the capabilities of the Q-MACS Etch system as infrared absorption and interferometer tool for on-line, in situ monitoring of molecular species and plasma etching rates in an industrial plasma-etching reactor used for semiconductor processing. For the first time, concentrations of the precursor gas NF_3 and of the etching product SiF_4 were measured on-line and in situ under clean room conditions. In addition, the etching rates of SiO_2 layers and of the silicon wafer were monitored, including plasma-etching endpoint detection.

The accuracy of concentration measurements of molecules in plasmas depends on the precision of available molecular data. For this purpose the absorption cross-sections of SiF_4 and NF_3 have been determined for the spectral range 1028 ± 0.3 cm^{-1}. Furthermore, the absorption cross-section of SiF_4 has been characterized as a function of temperature and pressure.

2. Absorption and Interferometry Background

2.1. Absorption

High spectral resolution (10^{-3} cm^{-1}) can be achieved using the IR-QCLAS technique. Individual vibration-rotation absorption lines can be measured, limited by Doppler and instrumental broadenings.

Under conditions of weak absorption, the radiation intensity, $I(\nu)$, transmitted through a homogeneous sample, is given by the Beer-Lambert law, Equation 1.

$$I(\nu) = I_0(\nu)\exp[-k(\nu)L] \tag{1}$$

$I_0(\nu)$ is the incident intensity, $k(\nu)$ the absorption coefficient, and L the absorption length. The integrated

 © 2007 WILEY-VCH Verlag GmbH & Co. KGaA, Weinheim

Chemical Vapor Deposition

value of the absorption coefficient, K_ν, is given by Equation 2.

$$K_\nu = \int_\nu k(\nu)d\nu = S(T)N \quad (2)$$

$S(T)$ is the line strength of a specific absorption line at the temperature T, and N is the total concentration of particles in all states. If the line strength (specific to each transition) is known, the total concentration of the species can be obtained.

SiF_4 measurements using absorption in the infrared spectral range have been reported for gas or plasma phase,[12–15] and also using a matrix isolation technique.[16] For NF_3, there are also reported measurements in the infrared spectral region.[17] Nakamura et al. determined, for the first time, the line strength measurement of SiF_4, using TDLAS with lead salt lasers, to be 4.2×10^{-20} cm molecule^{-1} at 1032.1 cm^{-1} at 380 K.[12] In IR, the SiF_4 ν_3 asymmetric bond stretching vibration lies at 1030.9 cm^{-1}. Due to the natural abundance of silicon (92.2 % (^{28}Si), 4.7 % (^{29}Si), and 3.1 % (^{30}Si)) and the large number of hot bands ($\nu_3 + n\nu_4 - \nu_4$) which overlap with the ν_3 band, the measured spectra at room temperature could not be spectrally resolved.[16] The recorded spectrum is complex, consisting of plenty of absorption lines that overlap. Even with the resolution of TDLAS (10^{-4} cm^{-1}), single lines could not be resolved. The peak absorbance at 1032.1 cm^{-1}, obtained from the literature,[13] is used to determine an effective line strength.

For unresolved spectra, the absorption cross-section is more appropriate to use. Equation 1 can be rewritten as Equation 3.

$$I(\nu) = I_0(\nu)\exp[-\sigma(\nu)\,N\,L] \quad (3)$$

$\sigma(\nu)$ is the absorption cross-section [cm^2 molecule^{-1}]. The absorption cross-section is defined for a spectral position and depends on temperature and pressure. If the particle density is known, then $\sigma(\nu)$ can be obtained from Equation 4.

$$\sigma(\nu) = \frac{\ln\left(\frac{I_0}{I}\right)_\nu}{N\,L} \quad (4)$$

2.2. Interferometry

In the case of the interference of the two reflected waves from a thin film, the optical path difference is given by Equation 5.

$$\Delta l = 2\,n\,d\,\cos(\beta) \quad (5)$$

n is the refractive index of the thin film material, and d is the thickness. At normal incidence, the refractive angle $\beta = 0°$. The optical path difference leads to a phase difference of the waves, shown in Equation 6.

$$\phi = 2\pi\Delta l / \lambda \quad (6)$$

λ is the probing laser wavelength. The reflected waves will interfere constructively whenever they are in phase, and destructively when they are in opposite phase. Each time that ϕ is an integer value of π, we have a maximum or a minimum of intensity. The interference condition for the thin film is then given by Equation 7.

$$2\,n\,d = m\,\lambda \quad (7)$$

Whenever $m = k$ and $k = 0, 1, 2, 3 ....$, the reflected intensity will show a maximum (constructive interference); for $m = k - \frac{1}{2}$ and $k = 1, 2, 3 ....$, the reflected intensity will show a minimum (destructive interference). Specific for an etched hole, the interference condition is satisfied by the $2\,d = m\,\lambda$, the optical path difference being just $2d$ ($n_{air} = 1$).

In fact, a series of multiple reflections are established inside a thin layer. The situation can be described by a multi-beam interference system where the reflected intensity is characterized by the Airey formulae, given by Equation 8.[4,18]

$$I_R(\phi) = \frac{I_0 F \sin 2(\phi/2)}{1 + F \sin 2(\phi/2)} \quad (8)$$

I_0 is the incidence intensity,$F = 4R/(1 - R)2$, and R is the reflectivity of the film interface. The reflectivity at normal incidence is given by Equation 9.

$$R = [(n - 1)/(n + 1)]^2 \quad (9)$$

In the case of etching a thin layer, as the thickness changes during the etch process, the reflected intensity oscillates following Equation 8, absorption and diffusion in the material or at the surface being neglected. The frequency of the oscillations is determined by the thickness variation and the laser probe wavelength. The shape and the amplitude of the reflected beam are determined by the reflectivity of the film interface. In Figure 1, the interfero-

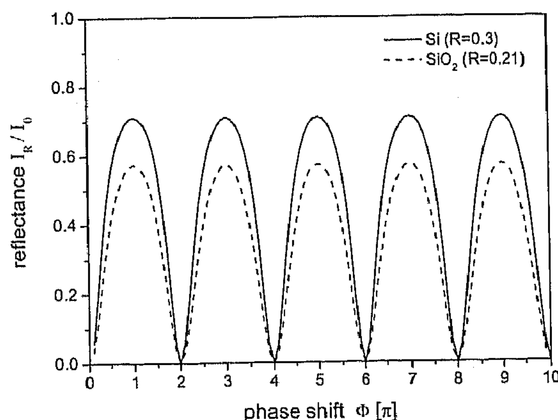

Fig. 1. Calculated reflected intensity function of the phase shift for Si and SiO_2 layers.

 © 2007 WILEY-VCH Verlag GmbH & Co. KGaA, Weinheim

gram for Si and SiO_2 is shown. The curves were calculated using the refractive index (n) for these materials at $\lambda = 9.7$ µm, which is the laser wavelength used here. The values which were considered here for the processed wafer material, taking into account the dependences for various porosities of the material, were measured at Qimonda with 3.42 and 2.75, respectively.[19]

3. Results and Discussions

3.1. General Spectroscopic Issues

The selection of the wavelength range for monitoring purposes in plasmas depends on several requirements and needs special attention. At first, the position and possible overlapping between ro-vibronic bands of the molecular plasma species of interest and the strength of the vibrational bands have to be known. Also needing to be considered are the availability of (i) QCLs in the MIR spectra region, (ii) thermoelectrically (TE) cooled detectors with high sensitivity and band width, and (iii) IR fibers with appropriate transmission and mechanical quality.

Two FTIR spectra recorded with a Bruker IFS 66 v/s spectrometer are shown in Figure 2. The spectra were recorded at room temperature in a gas cell of length 15 cm. The pressure in the cell was 0.5 mbar for SiF_4 and 1 mbar for NF_3. In our approach we want to measure the etch product SiF_4, with NF_3 being the precursor. The spectra of these species overlap. However, in order to measure the etch product SiF_4, minimum overlapping has to be considered. The spectral region 1028 ± 0.3 cm^{-1} was chosen for the measurement of SiF_4 because its absorption cross-section is about 90 times larger compared to NF_3. Other IR active vibrational modes of SiF_4 are found at larger wavelength values[18] where no QCLs are available. Hence, the choice was limited to detection of the ν_3 fundamental band.

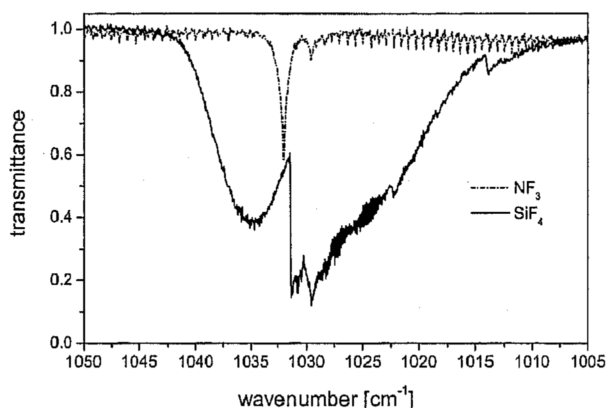

Fig. 2. FTIR spectra of SiF_4 under 0.5 mbar pressure and of NF_3 under 1 mbar pressure. The spectra were recorded at room temperature, at a total absorption length of 15 cm and spectral resolution of 0.11 cm^{-1}.

A reference spectrum of C_2H_4, recorded using Q-MACS Etch for an absorption length of 15 cm and under a pressure of 3 mbar at room temperature, is shown in Figure 3. The reference and the Ge etalon spectra were used for the wavelength calibration of the QCL spectrometer. The line profiles have a Doppler contribution, for which the full width at half maximum (FWHM) is given by

$$\Delta W_{\text{Doppler}} = 7.16 \times 10^{-7} \nu_0 \sqrt{\frac{T}{M}} \qquad (10)$$

where ν_0 is the wavenumber of the central line, T is the temperature, and M is the molar mass of the molecule. For the lines shown in Figure 3, Doppler broadening is about 2.4×10^{-3} cm^{-1}, calculated for room temperature. Another broadening effect, contributing to the profile, is the pressure broadening. From the HITRAN data base, pressure broadening of these lines are shown to be about 3×10^{-4} cm^{-1}.[20] The instrumental contribution to the laser lines was obtained after deconvolution of the absorbance profiles. The measured absorption lines show an instrumental broadening (FWHM) of about 8×10^{-3} cm^{-1}, which is therefore the dominating broadening effect of the lines.

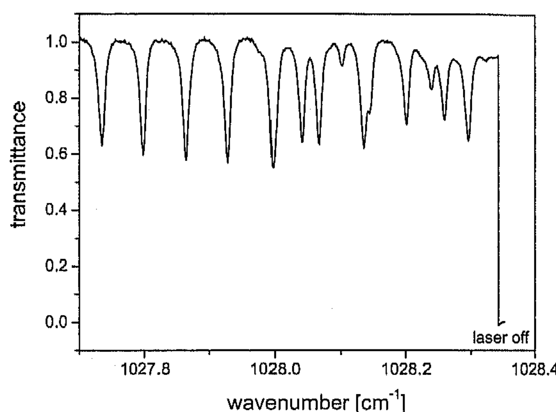

Fig. 3. QCLAS spectrum of C_2H_4 at room temperature, under 3 mbar pressure, with absorption length of 15 cm and instrumental broadening of 0.008 cm^{-1}.

The complex spectrum of SiF_4 is shown in Figure 4. It was recorded using Q-MACS Etch at a gas temperature of 70 °C in a gas mixture with 90 % of Ar. The total pressure was 0.333 mbar. The measurement has been done in the MERIE plasma reactor, where an absorption length of 108 cm was achieved in two passes. The same spectral region has been recorded using NF_3 in the gas phase under 0.8 mbar. Figure 5 shows the recorded NF_3 QCLAS spectrum. The NF_3 pattern is different to that of SiF_4, showing also an unresolved structure.

It should be emphasized that for the use of QCLs as radiation sources for molecular spectroscopy, in particular under low-pressure conditions, some differences compared to the application of lead salt lasers have to be considered: (i) due to higher power density, values of QCLs saturation ef-

 © 2007 WILEY-VCH Verlag GmbH & Co. KGaA, Weinheim

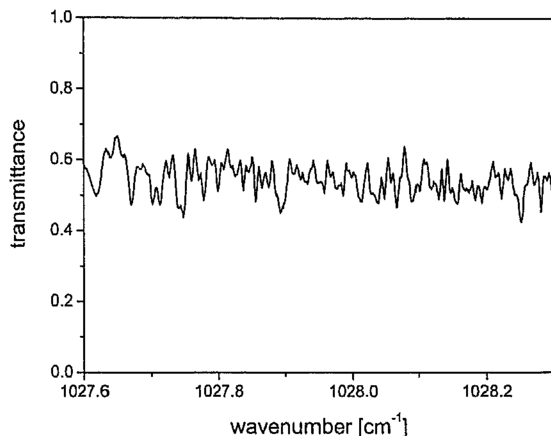

Fig. 4. QCLAS spectrum of 10 % SiF_4 in mixture with Ar, measured at 70 °C, under 0.333 mbar total pressure, with absorption length of 108 cm and instrumental broadening of 0.008 cm^{-1}.

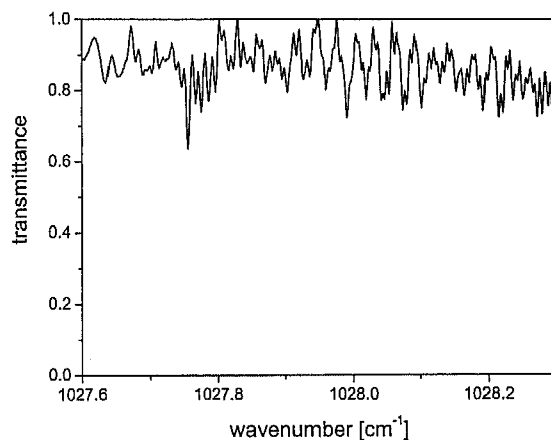

Fig. 5. QCLAS spectrum of NF_3 measured at 70 °C, under 0.8 mbar pressure, with absorption length of 108 cm and instrumental broadening of 0.008 cm^{-1}.

fects in the excitation of molecular levels may appear; (ii) the fast tuning of QCLs over the absorption lines, in scale of nanoseconds, can lead to rapid passage effects.[21] Both effects can cause an underestimation of measured concentrations. Consequently, all these effects have been carefully considered here for concentration measurement.

3.2. Determination of Absorption Cross-sections

Nakamura et al. demonstrated that SiF_4 behaves as an ideal gas, and provided measurements of the line strength.[12] It is known that the line strength of a rovibronic transition strongly depends on temperature.[22] Small variations in the temperature can lead to large changes of the population distribution over the rovibronic structure of the molecule, i.e., to changes of the total partition function. Therefore the dependence of the absorption cross-sections of SiF_4 on temperature and pressure has been determined experimentally. The SiF_4 absorbance function of the concentration is plotted in Figure 6. The gas temperature was varied between 60 to 110 °C by electrically heating the reactor walls. The pressure and hence the concentration was

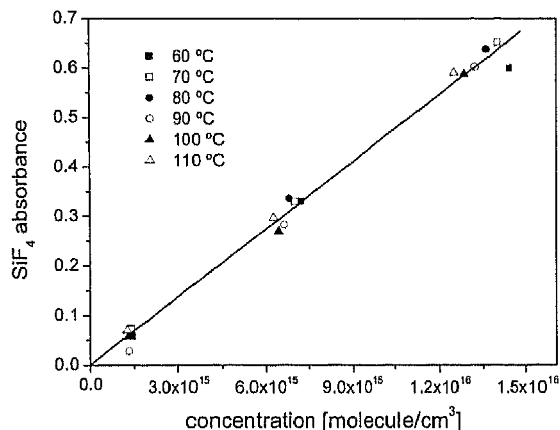

Fig. 6. SiF_4 average absorbance as a function of the concentration. The spectral region measured was 1027.6–1028.3 cm^{-1}, and the absorption length was 6 cm.

changed from 0.066 to 0.333, and further to 0.666 mbar. The absorption length was 6 cm. If the absorbance, $\ln(I_0/I)$, (see Eq. 4) is represented as function of the concentration, then the proportionality factor is the product σ L. From Figure 6 it can be seen that the data points can be linearly fitted. This shows that the absorption cross-section is constant over the range of temperature and pressure used in the experiment. Since we are working under relatively low pressures, the pressure broadening effects are negligible. The main contribution to the absorption profiles is the instrumental broadening which is about six times larger than the Doppler broadening, $\Delta W_{Doppler} = 1.24 \times 10^{-3} cm^{-1}$ for SiF_4 at room temperature. Recording complex spectra, the integrated absorption coefficient is evaluated over a large number of absorption lines, where the total partition function is less sensitive to the changes of the temperature as in the case of a single line.

The values of absorption cross sections have been obtained from either FTIR or QCLAS spectra. The average absorption cross-section at 1028 ± 0.3 cm^{-1} was measured to be $\sigma = (7.7 \pm 0.7) \times 10^{-18}$ cm^2 $molecule^{-1}$ for SiF_4, and $\sigma = (8.7 \pm 0.8) \times 10^{-20}$ cm^2 $molecule^{-1}$ for NF_3. Uncertainties are due to errors in the measurement of pressure and further of the I_0 reference.

3.3. Test of Validity

To prove the validity of the experimental approach, the first tests have focused on concentration measurements of SiF_4 in the gas phase. For this purpose, the mixing ratio of SiF_4 and Ar has been changed stepwise: 1, 2, 3, 4, 5, 10, 15,

© 2007 WILEY-VCH Verlag GmbH & Co. KGaA, Weinheim

20 % of SiF_4 in Ar. Results of these experiments are shown in Figure 7. The measurements have been performed under a total pressure of 0.333 mbar in the MERIE reactor. The concentration values result from the fitting of complex

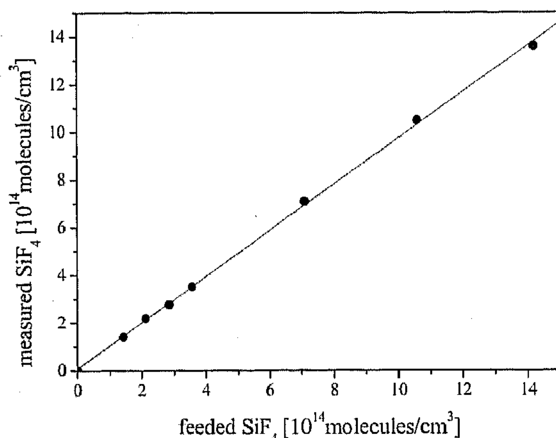

Fig. 7. Comparison of SiF_4 concentrations measured using the absorption cross-section and the values measured with flowmeters. The amount of SiF_4 fed is calculated from selected mixing ratios SiF_4/Ar of 1, 2, 3, 4, 5, 10, 15, 20:100 in the gas phase at room temperature and under a total pressure of 0.333 mbar.

spectra.[23] The absorbance area is measured and, based on Equation 3, an absolute concentration is determined using the measured values for the line strengths. This value is then converted in terms of a mixing ratio, i.e., part per billion (ppb), using the known temperature and total gas pressure. Due to the uniformity of the complex spectrum of SiF_4 at 1028 ± 0.3 cm^{-1}, an average absorption level could be used to derive the concentration. An average absorbance is obtained by measuring a reference signal for the case where no SiF_4 and NF_3 concentration are present, and the average intensity in the plasma phase. Based on Equation 4, absolute concentration can be determined by using the measured values of the respective absorption cross-section. Following the above procedure yields the same concentration values as those obtained from fitting the complex spectra. Figure 7 shows the concentration determined with the QCL system precisely matches the expected values for the given gas mixture. Thus, the QCLAS system can be very useful for a calibration of mass flow controllers. The limit of detection (LOD) of the Q-MACS Etch system for this configuration was found to be 300–3000 parts per million (ppm), depending on the total pressure under which the measurements were performed, i.e., 0.066–0.66 mbar. In terms of concentration the LOD was about 4×10^{12} molecule cm^{-3}.

3.4. Monitoring of Etch Processes

A typical example for monitoring etch processes via top-down access experiments is shown in Figure 8. Stable plas-

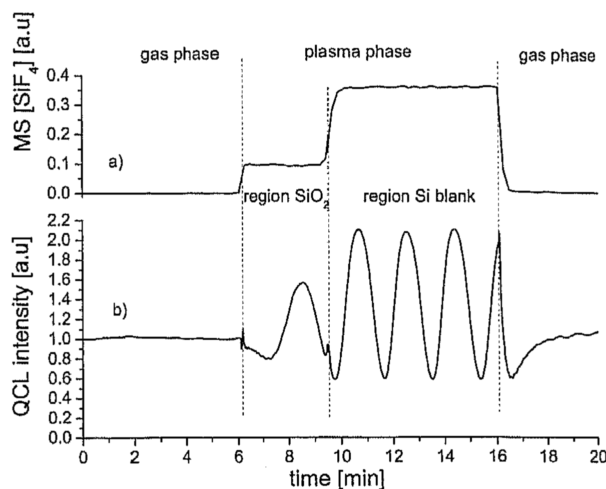

Fig. 8. Monitoring of the etching processes on a silicon oxide wafer. a) Time dependence of the SiF_4 mass spectrometer (MS) signal. b) Time dependence of the IR signal reflected at the wafer surface (QCLAS). Gas phase, Ar under 0.333 mbar. Plasma phase, 20 % Ar + 80 % NF_3 under 0.333 mbar total pressure.

ma conditions were chosen to etch a silicon oxide wafer with a layer thickness of several 100 nm. The feed gas mixture was 20 % Ar + 80 % NF_3, under at a total pressure of 0.333 mbar. The SiF_4 signal measured with a mass spectrometer is shown in Figure 8a. It can be seen that the concentration of SiF_4 considerably increases when etching reaches the silicon surface after complete removal of the SiO_2 layer.

The transition from SiO_2 to the silicon substrate can also be observed in the fringe spectra recorded with the Q-MACS Etch used as an interferometer system (Fig. 8b). The amplitude of the fringes is smaller for the case in which the interferogram results from interference effects on the SiO_2 layer. This is caused by the different refractive indexes of the materials leading to different reflectivities. Figure 1 shows the amplitude of the calculated fringes being lower for the interference on SiO_2 compared to that on silicon. The different absorbance and thickness of the materials leads to an offset in the interferogram, this effect can be observed in the measured signal. It is known that the absorbance of SiO_2 at the wavelength of 1028 cm^{-1} is about four orders of magnitude larger than that of Si.[4,24] Therefore, a thick layer of SiO_2, in the range of millimeters, is completely opaque and no interference can be observed. This is not the case for Si being IR-transparent, where an interferogram can be recorded for even substantially thick substrates. The absorption length for the top-down access is only 6 cm, and therefore the intensity loss due to SiF_4 absorption formed in the plasma is negligible.

The frequency of the fringes provides the information of the corresponding etch rate. Knowing the interference condition for Si and SiO_2 layers, and counting the number of fringes in time, the etch rate is obtained. Comparing the etch rates for Si and SiO_2, the etch rate is clearly higher for the silicon substrate. From the experimental data an etch

 © 2007 WILEY-VCH Verlag GmbH & Co. KGaA, Weinheim

rate of 800 nm min^{-1} for the silicon substrate, and 600 nm min^{-1} for the SiO_2 layer, were obtained. The error in measuring the etch rate of SiO_2 was higher because no complete fringe feature could be recorded, since the SiO_2 layer is just a couple of hundreds of nanometers thick. These etch rates were essentially the same as those obtained from balancing. Comparison between gravimetry and IR measurements reveals a difference of about 10 % for both methods. The differences can be explained by the fact that QCL interferometer results from a local measurement, i.e., an area of 1 cm diameter from the wafer center is measured, whereas balancing the wafer after the etch process has finished means a global average etch rate measurement.

Certainly, because of the shorter wavelength, the precision for an etch rate determination using a visible laser is higher compared to a IR-based method. The advantage of using IR interferometry was shown by Heason and Spencer.[4] For some materials interferometric measurements can not be done using the visible region due to very large absorbance inside the material.[24] Thus, a middle or near IR interferometer would be the choice for determination of a layer thickness. The interferometer can be used further for depth measurements of etched holes. However, due to the long wavelength used for IR this is only suitable for holes with large diameters. In the case of deep-trench etching, the diameter of the holes is on the scale of 100 nm or even smaller, leading to a diffraction of the IR beam. Thus, no fringes pattern containing depth information can be obtained.

Phase, amplitude, and frequency of the fringes are parameters which change with the layer material being etched. Therefore, the Q-MACS Etch interferometric system can also be used for end-point monitoring in top-down access.

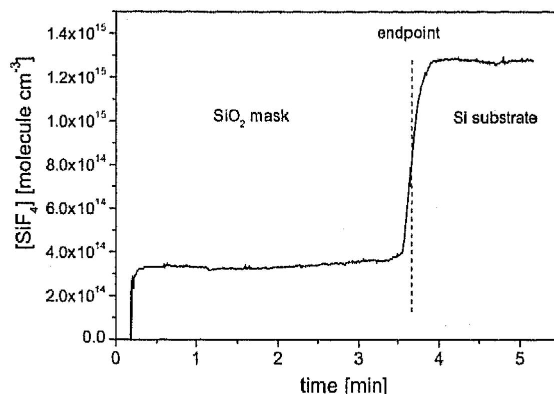

Fig. 9. SiF_4 concentration measurement using QCLAS in the process of etching a SiO_2 wafer. Plasma parameters; Ar 20 %, NF_3 80 % under 0.333 mbar total pressure.

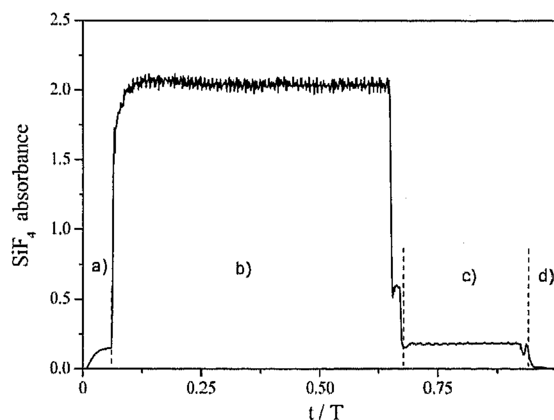

Fig. 10. SiF_4 absorbance monitoring using QCLAS for a complete cleaning process of the plasma etching reactor. a) and c) NF_3 gas phase, b) plasma phase, d) Ar gas phase. For the cleaning procedure a single-crystal silicon wafer was used.

3.5. Monitoring of SiF_4 Concentrations

The capability of Q-MACS Etch for SiF_4 concentration monitoring via side access is shown in Figure 9. The plasma parameters were the same as in previous experiments. The concentration of SiF_4 has been monitored during etching a silicon oxide wafer in an NF_3 plasma environment. A large increase in the SiF_4 concentration can be seen after the SiO_2 layer is completely removed.

As with the work of Sun et al.,[5] where TDLAS was used for SiF_4 concentration monitoring, here QCLAS proves to be a valuable and further enhanced tool for end-point detection in plasma-etch processes.

Another example of on-line in situ monitoring of the SiF_4 absorbance, $\ln(I_0/I)$, is shown in Figure 10. The SiF_4 concentration was monitored during a complete dry clean process using a single-crystal silicon wafer. During the first forty seconds, the NF_3 gas in the mixture with Ar is fed into the reactor. The small signals shown in the regions a) and c) are due to absorption of NF_3. For the region b), the signal is due to absorption of SiF_4 molecules in the plasma phase. The etch product SiF_4 is formed during etching of silicon in the highly reactive fluorine environment. In the plasma phase, the absorbance signal is about ten times higher compared to the gas phase and shows variations of the concentration of about 5 %. These variations have a frequency of 0.5 Hz, and are due to local variations of the plasma density caused by the influence of the applied magnetic field. In MERIE, the magnetic field was generated by four coils. Two adjacent coils were switched on consecutively, with the other two being switched off during the same time interval. With a frequency of 0.25 Hz all coils were alternatively activated in such a way that the plasma rotates, sweeping over the wafer surface. At moment d) the reactor is fed just with Ar. During the complete clean process few changes of pressure and power are made.

The selectivity of the measurement is limited due to the overlapping of NF_3 and SiF_4 spectra. A small contribution of NF_3 to the absorption signal can be expected. Without any dissociation of NF_3 the upper limit would be about

© 2007 WILEY-VCH Verlag GmbH & Co. KGaA, Weinheim

10 % of the whole absorption. Due to the dissociation of the NF_3 molecules in the plasma, the error in SiF_4 concentrations measurements caused by the absorption of remaining NF_3 can be neglected.

An example of on-line, in situ monitoring of the SiF_4 absorbance during a deep-trench etch process is shown in Figure 11. In order to prove the selectivity and sensitivity of the measurement, the experiment has been repeated (Fig. 11, curves a and b). In the second experiment (Fig. 11, curve b), 2 % of SiF_4 has been added to the plasma after about 10 min of the total recorded process time.

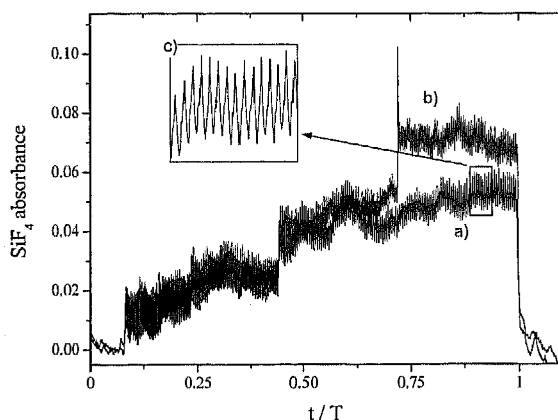

Fig. 11. SiF_4 absorbance monitoring QCLAS for: a) a complete plasma-etching process; b) complete plasma-etching process with injection of 2 % SiF_4; c) SiF_4 concentration variation due to changes of the magnetic field. The experiments were performed with a process wafer.

When comparing the curves a and b in Figure 11, a step jump in the concentration due to SiF_4 injection can be clearly seen. Figure 11c shows the enlarged temporal behavior of the measured concentration. Changes of the concentration due to plasma density over the wafer are clearly visible and further prove the sensitivity and time resolution of the method.

4. Summary and Conclusions

For the first time, in industrial etching plasmas used for semiconductor processing, concentrations of the precursor gas NF_3 and of the etch product SiF_4 were measured online and in situ. For this purpose, a new compact diagnostic arrangement, the Q-MACS Etch system, which is based on quantum cascade laser absorption spectroscopy and interferometry, has been designed and constructed. The Q-MACS Etch system provides high sensitivity and long term stability, because in addition to the measuring channel used in the plasma chamber, a reference and a pulse normalization channel are included. For simple operation and the avoidance of open optical pathways, an optical coupling with a MIR fiber to the plasma reactor has been realized. Using internal reflections, provided by a retro-reflector, only one optical access window is necessary. Adapted to clean room requirements and for a low maintenance level, thermoelectric cooled detectors are used on board.

With Q-MACS Etch the etch rates of SiO_2 layers and of the silicon wafer were monitored. The QCL system has shown its capabilities for plasma-etching, end-point detection and for mass flow controller calibration. The experiments have been performed in an industrial, dual-frequency, capacitively coupled, magnetically enhanced, reactive ion etcher (MERIE), which is a plasma reactor developed for DRAM technologies.

To achieve a sufficient accuracy of concentration measurements, the absorption cross-sections of NF_3 and SiF_4 have been determined. The temperature and pressure dependence of the cross-sections have been proven. In the spectral range 1028 ± 0.3 cm^{-1} the absorption cross-sections of SiF_4 and NF_3 have been determined to be $\sigma = (7.7 \pm 0.7) \times 10^{-18}$ cm^2 $molecule^{-1}$ and $\sigma = (8.7 \pm 0.8) \times 10^{-20}$ cm^2 $molecule^{-1}$, respectively.

The first application of a QCL arrangement for monitoring of industrial etch processes has opened up a challenging new option for control of demanding semiconductor production. Focused on sensitive and fast concentration measurements of molecular key components, while ensuring compactness, robustness, and long term stability, this new class of process control equipment has the potential to become implemented also into other fields of plasma technology.

5. Experimental

Plasma Reactor: A dual-frequency, capacitively coupled, magnetically enhanced, reactive ion-etch plasma reactor (DF CCP MERIE) (see Fig. 12), which is an improved version of a conventional reactive ion-etch system,[25] was used for the experiments. A 60 MHz source power generator was used to sustain the plasma and control the plasma density, enabling power levels up to 3.5 kW to be applied. A 2 MHz bias power generator enabled up to 3 kW to be applied, and was used to control the ion energy. With the combination of a high- and low-frequency drive, independent control of plasma density (and hence ion flux) and ion energy was obtained, this being a major advantage in regards to conventional RIE systems. Furthermore, a DC magnetic field in the range 0–120 G can be imposed parallel to the surface of the RF-powered electrode. The B-field yielded an increased plasma density and reduced the sheath voltage. As a result a higher flux of ions with lower energy could be obtained.

The substrate to be etched was placed on the powered electrode, whereas the opposite electrode was grounded. Ions generated in the plasma bulk were accelerated towards the wafer by the sheath fields, which subsequently led to an enhanced etch process at the wafer surface. The plasma etch products and feed gases were constantly removed by a turbo pump. The plasma pressure was varied in the range 0.08–0.8 mbar, and the total flow was in the range 50–1000 sccm. The feedstock gas selection was controlled by the etch process requirements in regards on the materials to be etched, etch rate, anisotropy, and selectivity. For our experiment we used HBr, NF_3, O_2, Ar, He, SiF_4, and $SiCl_4$ as feed gases.

The Q-MACS Etch System: The quantum cascade laser system Q-MACS Etch consists of a pulsed infrared QCL source with the laser wavelength tunable in the range 1027–1032 cm^{-1}, optical components, detectors, and data acquisition cards controlled by a PC. Figure 13 shows a photo of the Q-MACS Etch system. Details of the optical arrangement inside the black box are shown in Figure 14. The laser driver used was a Q-MACS Basic [10,11]. The Q-MACS Basic provides a laser pulse width tunable in the

 © 2007 WILEY-VCH Verlag GmbH & Co. KGaA, Weinheim

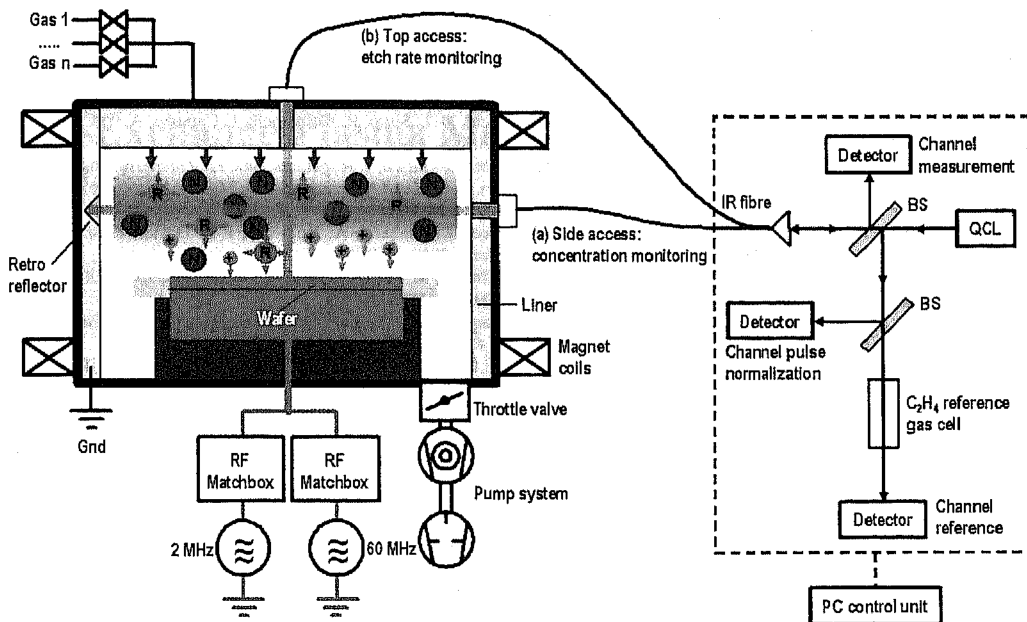

Fig. 12. Experimental arrangement of the MERIE plasma-etching reactor and the 3 channel Q-MACS Etch system: a) side access; b) top down access.

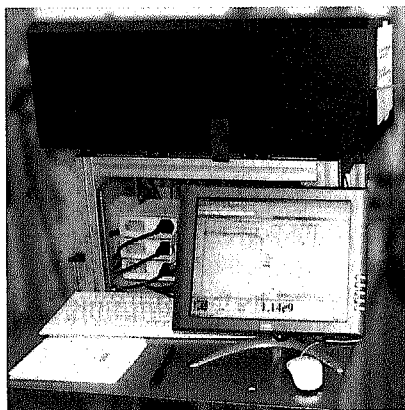

Fig. 13. Photograph of the Q-MACS Etch system.

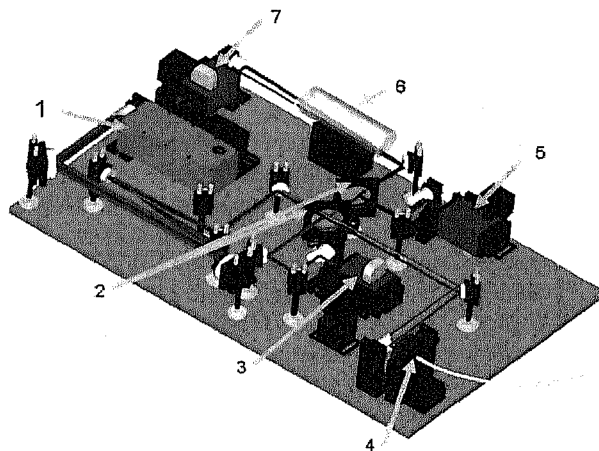

Fig. 14. Scheme of the optical arrangement of the Q-MACS Etch system (1, laser head; 2, beam splitters; 3, 5, 7, detectors; 4, IR optical fiber; 6, reference gas cell).

range 10–255 ns, and a repetition frequency in the range 100 Hz–1 MHz. The system can operate in the *intra pulse* or in the *inter pulse* mode, depending on the experimental requirements [10]. Intra pulse mode means that the laser frequency is tuned over the absorption spectrum during one relatively long single pulse, i.e., using 50–200 ns laser pulse width.

In the present experiments the inter pulse mode has been used. The QCL was driven with a pulse width of 12 ns and a repetition rate of 500 kHz. The central frequency of the QCL was chosen by changing the working temperature between −30 to +30 °C and the feed current of the laser in the range 0.5–15 A (peak current). In order to tune over a spectral range, an additional voltage ramp was applied to the laser with a frequency of 1 kHz. This allows scanning of the spectral range with a width of up to one wavenumber. Each millisecond a complete spectral region was scanned. Under each scan, 500 single laser pulses were generated. As result the measured spectrum with a time resolution of 1 s was an average of a thousand spectra. One second time resolution is sufficient for most plasma etch processes which require a time scale typically in the range of seconds up to minutes.

From Figures 12 and 14 it can be seen that the IR beam was split into three channels using two IR transparent ZnSe beam splitters (BS). The main part of the beam was coupled into an IR fiber using an off-axis parabolic (OAP) mirror, and then collimated into the plasma reactor using either lenses or OAPs. The second channel, operating as pulse normalization channel, was used to reduce the fluctuation intensities of the QCL from pulse to pulse. In the third channel a reference spectrum of C_2H_4 was measured through a reference gas cell in order to calibrate the spectral region and to correct drifts of the laser frequency due to temperature instability of the laser chip. For the spectral calibration a Ge etalon with the free spectral range of 0.012 cm^{-1} was used. A fringe spectrum was recorded and used to correct the nonlinearity of the spectral laser tuning. Together with the known spectra of the C_2H_4 absolute spectral calibration has been performed [20].

Industrial requirements, such as no open optical path and the availability of just one optical port access, make the infrared beam coupling into the reactor a challenging task. The solution presented here is based on the use of middle infrared fibers and internal reflections in the reactor chamber. Two types of experimental set-ups have been utilized. Figure 12a shows a side ac-

 © 2007 WILEY-VCH Verlag GmbH & Co. KGaA, Weinheim

cess configuration used for concentration measurements, whilst Figure 12b shows the top-down access arrangement used for interferometer measurements. In both cases, the IR laser beam is guided using one meter long IR fiber with anti-reflection treatment of the fiber ends for the specific laser wavelength. The IR fibers are made of AgCl/AgBr materials. The laser has been collimated into the plasma reactor using an OAP for the side access and a ZnSe lens for the top-down access. In case (a), the beam was reflected back using a retro-reflector installed at the plasma chamber wall. For the top-down arrangement the wafer itself was used as the reflector. The reflected beam was coupled into the same path and reached the measurement detector using the second beam splitter (BS) in reflection mode.

Unfortunately, an important part of the intensity of the measurement signal is lost in the transmission mode of the BS. Sternheim et al. have already tried to avoid this effect [3]. They described an effective coupling of the radiation of a HeNe laser using an active medium such as $\lambda/4$ plate which rotates the polarization plan. The BS works for the incoming beam in transmission and for the outgoing beam in reflection. In our case, the radiation of the QCL is linearly polarized, but after passing the IR fiber the beam is nearly non-polarized. Unfortunately, mid-IR fibers preserving a polarization are not yet available commercially. Therefore, we could not use the elegant approach of Sternheim et al. [3].

In both sets of experiments three types of wafers, single-crystal silicon, silicon oxide, and process wafers, have been used. In the case of silicon oxide and process wafers, additional layers were coated on the substrate of single-crystal silicon material. On top of the silicon substrate, with thickness of about 1 mm, the silicon oxide layer had a thickness of several 100 nm. The process wafers were masked for the deep trench etch process used for fabrication of DRAM.

Received: October 30, 2006
Revised: April 1, 2007

[1] A. Steinbach, S. Barth, A. Henke, S. Wege, J. Sobe, M. Reinicke, M. Kijowski, *Proc. 6th Eur. Conf. Adv. Eqpt. Control/Adv. Process Control*, European AEC/APC Committee, Dublin **2005**

[2] W. Grählert, I. Dani, O.Throl, V. Hopfe, K. Pietsch, T. Wünsche, T. Dreyer, *VDI-Berichte* **2006**, *19*, 45.

[3] M. Sternheim, W. van Gelder, A. W. Hartman, *J. Electrochem. Soc.: Solid-State Sci. Technol.* **1983**, *130*, 655.

[4] D. J. Heason, A. G. Spencer, *J. Phys. D: Appl. Phys.* **2003**, *36*, 1543.

[5] H. C. Sun, V. Patel, B. Singh, C. K. Ng, E. A. Whittaker, *Appl. Phys. Lett.* **1994**, *64*, 2779.

[6] J. Faist, F. Capasso, D. L. Sivco, C. Sirtori, A. L. Hutchinson, A. Cho, *Science* **1994**, *264*, 553.

[7] S. Blaser, *Proc. 4th Workshop on QCL Technology and Application* (Ed: K. Sassenscheid), FHG-IPM, Freiburg, Germany **2003**, p.22.

[8] M. Beck, *Proc. 4th Workshop on QCL Technology and Application*, (Ed: K. Sassenscheid), FHG-IPM, Freiburg, Germany **2003**, p.38.

[9] C. Gmachl, D. L. Sivco, R. Colombelli, F. Capasso, A. Y. Cho, *Nature* **2002**, *415*, 883.

[10] F. Hempel, S. Glitsch, J. Röpcke, S. Saß, H. Zimmermann, in *Plasma Polymers and Related Materials* (Ed: M. Mutlu), Hacettepe University Press **2005**, p.142

[11] J. Röpcke, G. Lombardi, A. Rousseau, P. B. Davies, *Plasma Sources Sci. Technol.* **2006**, *15*, S148.

[12] M. Nakamura, M. Hori, T. Goto, M. Ito, N. Ishii, *Jpn. J. Appl. Phys., Part 1* **2001**, *40*, 4730.

[13] A. A. Langford, B. P. Nelson, M. L. Fleet, R. S. Crandall, *Phys. Review B.* **1990**, *42*, 7245.

[14] T. Ohta, K. Hara, T. Ishida, M. Hori, T. Goto, M. Ito, S. Kawakami, N. Ishii, *J. Appl. Phys., Part 1* **2003**, *94*, 1428.

[15] T. Ohta, M. Hori, T. Ishida, T. Goto, M. Ito, S. Kawakami, N. Ishii, *Jpn. J. Appl. Phys., Part 2* **2003**, *42*, L1532.

[16] F. Königer, A. Müller, W. J. Orville-Thomas, *J. Mol. Struct.* **1977**, *37*, 199.

[17] M. W. Chase, Jr., *J. Phys. Chem. Ref. Data, Monograph* **1998**, *9*, pp. 1–1951.

[18] W. Demtröder, *Laser Spectroscopy, 3rd Edition*, Springer-Verlag, Berlin **2003**.

[19] Qimonda GmbH & Co, internal measurements, private communication.

[20] R. R. Gamache, A. Goldman, L. S. Rothman, *Quant. Spectr. Rad. Transf.* **1998**, *59*, 495.

[21] G. Duxbury, N. Langford, M. T. McCulloch, S. Wright, *Chem. Soc. Rev.* **2005**, *34*, 921.

[22] G. D. Stancu, J. Röpcke, P. B. Davies, *J. Chem. Phys.* **2005**, *122*, 014306.

[23] C. Harward, F. Hempel, J. Röpcke, H. Zimmermann, *Proc. 1st Int. Workshop Infrared Plasma Spectroscopy*, INP, Greifswald, Germany **2006**.

[24] D. R. Lide, *Handbook of Chemistry and Physics*, 86th Edition, Taylor and Francis, London **2005**.

[25] S. Wege, A. Steinbach, S. Barth, A. Henke, J. Sobe, M. Reinicke, J. W. Bartha, G. D. Stancu, N. Lang, J. Röpcke, in *Proc. AVS 53rd Int. Symp. & Exhibition* (Ed: T. Michalske), San Francisco **2006**, PS2-FrM4.

 © 2007 WILEY-VCH Verlag GmbH & Co. KGaA, Weinheim